

Analysis of the State Estimation Performance in Transient Conditions

Marija Zima-Bočkarjova, *Member, IEEE*, Marek Zima, *Senior Member, IEEE*, and Göran Andersson, *Fellow, IEEE*

Abstract—An accurate and reliable performance of a state estimation under all network conditions is crucial for the monitoring of power systems and thus their secure operation. State estimation is based on a static representation of the power system, although the most critical operation conditions occur when power system is in dynamic transition from one state to another.

We propose how the performance of a state estimator can be monitored, evaluated during dynamic conditions and which factors affect it most. Based on that, we propose a method, which can be used to guide upgrading of a state estimation infrastructure to improve the state estimator performance during dynamic conditions. We demonstrate our suggestions on a test system.

Index Terms—Measurements, power system dynamics, power system monitoring, power system planning, state estimation, trajectory sensitivities.

I. INTRODUCTION

STATE estimation is an essential tool in the operation of modern power systems. The objective of state estimation is to determine the most likely state of the power system, i.e., magnitudes and phase angles of voltages in all the nodes. As an input, state estimation uses the system model, the topology status collected from substations, and the most recent available measurements, which can be redundant and contain noise. Having the system state and the system model, all the active and reactive power flows in the system can be computed, even if these flows were not measured originally.

This information is either directly displayed to an operator supervising the power system or is further processed by other applications. Security assessment providing decision support to the operators, billing, such as determination of transmission losses, and settlements can be mentioned as examples of these applications. Steps in measurement acquisition and role of state estimation are shown in Fig. 1. It is usually executed in regular time intervals, typically from a few seconds up to several minutes.

Standard state estimators nowadays employ algorithms using static system modeling, first proposed by Schweppe *et al.* [1]–[3]. These methods based on static models assume that the system is in quasi steady state, which is necessary mostly due to the technological limitations of the measurement collection chain. However, underlying power system is in a permanent dynamic evolution of various time scales. In this context, static

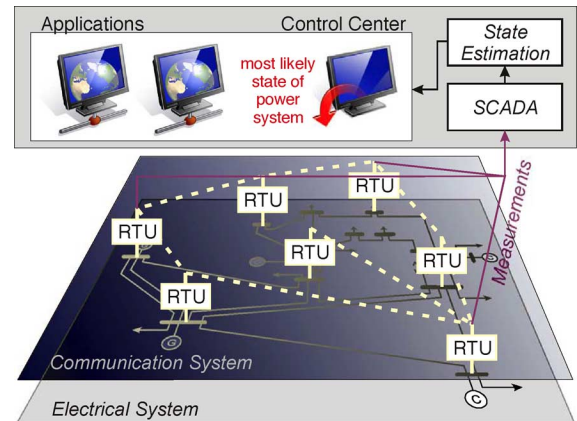


Fig. 1. Measurement acquisition and state estimation in power systems.

state estimators shall determine instantaneous algebraic state of the power system. Yet, the discrepancy between the results of state estimation and the underlying actual system state is strongly influenced by the quality/accuracy of the measurement chain, perhaps mostly by the so-called time skew of measurements.

The term time skew refers to the state estimator processing in a single snapshot measurements taken at different time instants. This phenomenon has two major sources:

- differing communication delays;
- the deadbands—thresholds of the signal changes being reported by the remote terminal units (RTUs).

The measurement infrastructure can vary within the same power system. The secondary technology used for the data collection differs from substation to substation as a consequence of many factors, equipment from different manufacturers, various equipment generations, etc. Besides, the communication infrastructure between substations and the network control center usually also vary. If the time skew and measurement inaccuracy is very significant, it may lead to the inability of the state estimation to converge and thus the inability to estimate the system state at all. This could leave system operators “blind”, without appropriate system information exactly at the moment when this information is critical, e.g., when the system undergoes dynamic changes, either these are caused by disturbances or just due to rapid changes implied by new schedule settings [4].

The problem of time skews could be solved with available nowadays technology, explicitly with the total replacement of the RTUs by the phasor measurement units (PMUs) [5]–[7]. These devices provide synchronous sampling with clock based on GPS signals. This would imply a very high accuracy measurements, whose time stamp information would eliminate the

Manuscript received November 26, 2009; revised April 11, 2010 and September 02, 2010; accepted January 04, 2011. Date of publication April 05, 2011; date of current version October 21, 2011. The work of M. Zima was supported by ABB Switzerland Ltd. Paper no. TPWRS-00921-2009.

The authors are with ETH Zürich, CH-8092 Zürich, Switzerland (e-mail: bockarjova@gmail.com).

Color versions of one or more of the figures in this paper are available online at <http://ieeexplore.ieee.org>.

Digital Object Identifier 10.1109/TPWRS.2011.2124476

problem with a different transmission time delay to the processing location (presumably state estimator in a control center). Few PMUs are installed in the systems. Despite obvious advantages, this technology is still far from massive deployment due to natural inertia for the renovation of the assets as well as measurement and control infrastructure. It is also associated with high manpower and financial investments, and it requires high bandwidth communications and a very powerful computer capable to process such large amount of data.

A. Terminology

Several papers have been published introducing what is called dynamic state estimation, where however the term dynamic was used in different contexts. Before proceeding, we find it appropriate to review the use of this term. Several publications refer to a static state estimation algorithm that solves problem in a shorter computational time as dynamic state estimation. Multi-snapshot recursive state estimators are also referred to as dynamic [8], [9]. These methods process sequential measurement snapshots and are combined [8] or not (tracking SE) [10] with various short-term, in the order of several minutes, load forecasting techniques to consider the slow variation of algebraic states.

Dynamic state estimators have been proposed to estimate power swings and associated states involving observer-based techniques [11]–[13]. The objective of the dynamic state estimation is in this case to determine the state from few nonredundant measurements and predict system evolution several seconds ahead.

In recent discussions and publications, dynamic state estimation gains more and more attention by the research community, not at least encouraged by the availability of the PMUs. Furthermore, there is a growing need for the fast flexible control systems. However, to our knowledge, no dynamic state estimators have been implemented in real power systems. Despite new attractive features, dynamic state estimators are associated with high computational complexity and necessity of adequate dynamic models of the power system.

However, we would like to stress that this paper does not suggest dynamic state estimation; instead, we focus on how static state estimation can be evaluated.

B. Contribution

In this paper, we refer to the dynamic performance of the traditional state estimator as to the performance during the *electromechanical transient* conditions, i.e., during power swings. Further, the measurement chain model proposed in this paper can also be applied in steady or quasi steady-state conditions.

There has been a lot of innovative work reported in the literature, dealing with state estimation [14], [15]. We would like especially to mention two publications, i.e., [16] and [17]. The ideas expressed in these papers are in our view an additional confirmation of the necessity of our presented work. In [16], sensitivity of the estimation error and voltage estimates with respect to voltage, injection and flow measurements, line parameters and measurement weights, in addition to the statistics of the sensitivities are determined for a number of static snapshots. The necessity to address dynamic response, both in the measurement and in the communication chain, is emphasized in [17].

The authors of [17] use constant time sampling of 20/200 ms and assume stochastic time delays with mean values of 0.0019 s in the 10-Mb/s Ethernet communication network. The system dynamics and the measurement chain noise are modeled by stochastic differential equations.

However, to our knowledge, the performance of a traditional state estimator based on a static model during system dynamics has not been studied in depth and a systematic analysis approach has not been proposed yet. We target our contribution to this topic by:

- 1) a concept for analysis of dynamic performance of state estimation;
- 2) an approach to improve state estimation performance during dynamic conditions by upgrading the SCADA infrastructure.

We believe that assessment of dynamic performance of a state estimator should be considered and even become a standard procedure in the engineering and parameterization of the state estimator. We propose methods for the suggested steps of the analysis, i.e., modeling of the SCADA for the state estimation purpose, evaluation of the dynamic performance, and how to practically use these results in SCADA upgrades.

We believe that the type of analysis we propose may contribute to, e.g., reduction of the time skew of measurements by recognizing which parameters of the measurement infrastructure contribute to it most.

C. Paper Organization

The paper is structured as follows. First, we describe a general dynamic model and introduce a measurement chain model. Then, the state estimation principle is briefly reviewed and a performance index is proposed to evaluate state estimation accuracy in the simulated conditions. An example demonstrates the necessity to analyze state estimation performance in the transient conditions. Then, we propose trajectory sensitivities to determine efficiently the influence of the parameters change. The sensitivity of the state estimation to the accuracy of the measurement chain components is shown in an example. Using these results, an approach to SCADA infrastructure enhancement is formulated. Summarizing remarks conclude the paper.

II. PROPOSED DYNAMIC ANALYSIS

A. Dynamic Power System Model

An efficient framework for modeling of nonlinear systems featuring discrete states has been presented in [18]. Its application on power systems modeling has been further shown in [19] and [20], where a natural flexible modular structure following power systems components classification has been introduced.

Applying the original formulation from [18], we can write a model of the power system dynamics in a compact form:

$$\dot{x} = f(x, y, z, \lambda) \quad (1)$$

$$0 = g^0(x, y, z, \lambda) \quad (2)$$

with the changes in g^0 due to the structural change of the power system, defined by

$$0 = \begin{cases} g^{i-}(x, y, z, \lambda) & y_{d,i} < 0 \\ g^{i+}(x, y, z, \lambda) & y_{d,i} > 0 \end{cases} \quad i = 1, \dots, d \quad (3)$$

and the discrete variable switchings

$$z^+ = h_j(x^-, y^-, z^-, \lambda)$$

$$y_{e,j} = 0 \quad j \in \{1, \dots, e\} \quad (4)$$

$$\dot{z} = 0 \quad y_{e,j} \neq 0 \quad j \in \{1, \dots, e\} \quad (5)$$

where

$$\begin{aligned} y_d &= Dy & x &\in X \subseteq \mathbf{R}^n & y &\in Y \subseteq \mathbf{R}^m \\ y_e &= Ey & z &\in Z \subseteq \mathbf{R}^k & \lambda &\in L \subseteq \mathbf{R}^l \end{aligned} \quad (6)$$

Differential variables are denoted x , algebraic variables y , and discrete state variables z . Switching of the status of discrete variables is governed by (4) when the corresponding auxiliary variables of y_e are equal to zero. Auxiliary variables y_d determine the region of validity of (3).

In power systems, this may be explained by the example of a line, which changes its status. When the line is in service, equations linking the current through the line and voltages at both ends of the line as well as line parameters, namely line impedance and shunt admittance, are valid. When the line is out of service, i.e., disconnected, current flowing through it is zero. The auxiliary variable is in that case the difference between the time and the instant when the line was tripped.

Further examples of hybrid dynamics in power systems are tap-changing transformers, excitation limiters, etc.

Matrices D and E are normally very sparse and their nonzero elements are equal to one on the positions corresponding to the auxiliary variables.

The above equations are solved numerically by employing, e.g., trapezoidal integration.

B. Proposed Measurement Chain Models

In this paper, we address SCADA chain from the measurement up to the state estimation consisting of the following components:

- instrument transformer(s);
- transducer (active and reactive power computation);
- RTU.

Adopting a convenient modular structure [19] for the framework of (1)–(6), each of the above listed components can be modeled as a module with internal variables and set of equations linked to other modules via external variables and coupling algebraic equations.

This flexible structure allows an individual choice of the model complexity for various components. For example, different types of RTUs with different sampling principles can be studied. Thus, also communication delays can be included in the modeling if desired. Our objective is to present an analysis method; therefore, we focus on other properties of the SCADA infrastructure, such as deadbands of RTUs, etc. and we neglect the topic of time delay in this paper.

We demonstrate the above modular modeling approach on an example of a current measurement transformer (CT). Accuracy classes of current measurement transformers are derived from their multiplicative error at the nominal value of the measured current. Their measurement error is higher for lower values of the measured current. However, in a simplified form, it can be assumed that the error of the measured current is constant for the entire measurement range. Further, if per-unit system is applied for the computations, the measured current on the sec-

ondary side equals the measured current on the primary side of the transformer in the absence of an error. If the measurement is biased by an error, the current on the secondary side of the CT is distorted proportionally to the error. Similar to [19] in our modeling, we adopted convention of expressing currents and voltages in a complex plane via their respective rectangular real and imaginary part coordinates. In accordance with (1)–(6), we define CT quantities as algebraic variables and the parameter

$$\begin{aligned} \lambda &: \epsilon \\ y_1 &: I'_{Re} \\ y_2 &: I'_{Im} \\ y_3 &: I'' \\ y_4 &: I''_{Re} \\ y_5 &: I''_{Im} \\ y_6 &: I'' \end{aligned} \quad (7)$$

where superscript $'$ refers to the primary and $''$ to the secondary transformer's side quantities. The parameter λ corresponds to the multiplicative error ϵ . Then it can be written

$$\begin{aligned} \lambda &: \epsilon \\ g_1 &: 0 = y_1^2 + y_2^2 - y_3^2 \\ g_2 &: 0 = y_1 \cdot (1 + \lambda) - y_4 \\ g_3 &: 0 = y_2 \cdot (1 + \lambda) - y_5 \\ g_4 &: 0 = y_3 \cdot (1 + \lambda) - y_6. \end{aligned} \quad (8)$$

The expressions $g_2 \dots g_4$ in (8) describe in terms of algebraic variables how the measured current on the primary side of the CT is biased by the measurement error and the expression g_1 how the RMS value of the primary side current is linked to its real and imaginary coordinates.

Two additional equations are necessary to link the above module/description to the corresponding primary equipment component, whose current is measured, in other words, how y_1 and y_2 are equal to the respective real and imaginary part of the current of a component (e.g., a line) whose current this CT measures.

Note that features of the framework (1)–(6) allowing the inclusion of a hybrid dynamics are necessary to enable modeling of an RTU. For details, please refer to Appendix A.

Any dynamic simulator of power systems can be augmented by introducing new models reproducing the measurement and data collection chains, i.e., the components directly giving input to the state estimation. Thus, the measurements o can be extracted from power system states available in the simulation model.

C. Evaluation of State Estimator Performance

The objective of a traditional state estimation [1]–[3] is to find the vector of states \hat{v} minimizing the value of the function J_{SE} , i.e., minimizing the deviation between observations and the estimated values

$$J_{SE} = \sum_{s=1}^S J_{SE,s} = \sum_{s=1}^S W_s \{o_s - h_s(\hat{v})\}^2 \quad (9)$$

where o is a measurement vector and \hat{v} is an estimated state vector.

The underlying assumption is that the system model (i.e., the structure of the functions $h_s(\cdot)$) as well as measurements o are known. In power system state estimation, o and v are commonly denoted as z and x , respectively. The new notations are introduced for consistency with the dynamic model (1)–(6). Note that the algebraic states v used in the state estimator (9) are a subset of y .

The value of the J_{SE} indirectly expresses how good the solution of the state estimation is, i.e., the fit between the measurements and linking of system states. This widely accepted index does not fully serve our purpose. Indeed it shows how well the determined state fits to the observations but it does not reflect how far from the reality the estimate is.

Contrary to that, we propose to quantify the performance of a state estimator during dynamic conditions with the index expressing a weighted deviation of the *measurements* from the actual conditions

$$J_p = \sum_{s=1}^S W_s (h_s(v) - o_s)^2. \quad (10)$$

In the following discussion, we refer to these deviations of the measurements from the actual conditions as the residuals. By actual conditions, we mean the values which can not be obtained in reality, i.e., known to the actual state estimator running online. But they are available in the simulation environment; therefore, they can be utilized for the analysis of the performance of a state estimator in dynamic conditions.

In other words, this index expresses how the system states, if they would be perfectly known or estimated, would map into measurements' equivalents via measurement functions.

The example in the next subsection demonstrates that J_{SE} is not a reliable indicator for the evaluation of the accuracy of a state estimator when a power system is subjected to dynamically changing conditions. However the proposed index J_p gives a better indication of this accuracy.

The above introduced index J_p can be obtained in the simulation environment by expanding the model introduced in Section II-B by two other types of modules:

- module for the computation of an individual residual;
- final module collecting all residuals.

The overall setup is shown in Fig. 2.

D. Illustrative Example

The nine-bus test system is described in Appendix A. As a benchmark scenario, we chose the trip of the line (C) 5.3 s after the beginning of the simulation, due to a fault or switching. It is assumed that the topology change is instantaneously corrected in the model. It is crucial that state estimation would provide a correct result as soon as possible, since especially in the case of such an event, the risk of an subsequent component outage due to an overload is higher.

The active and reactive power measurement errors induced by measurement chain are shown in Fig. 3; both the true value of the measured signal and the RTU output are shown for the line flow as well as squared residuals in the bottom plot, i.e., squared difference between the actual signal and the output of the RTU.

The top part of the figure provides a basis for an intuitive judgment of the impact of an RTU deadband on the time skew

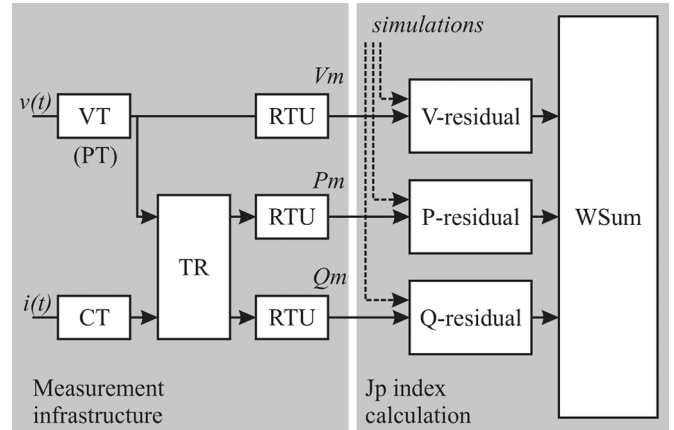


Fig. 2. Measurement infrastructure and performance index calculation proposed for the state estimation performance evaluation in dynamic conditions. TR denotes transducer, V_m , P_m , Q_m are the measurements. Residual calculation module uses simulated ideal measurements. The weighted sum (WSum) is a module collecting all residuals.

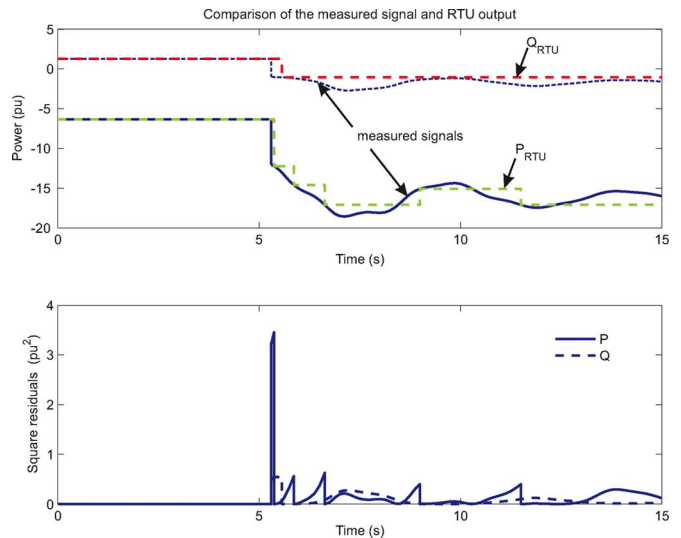


Fig. 3. Top part of the figure shows how the active and reactive power flows are reproduced by the part of the measurement chain consisting of the CT, VT, transducer, and RTU. The residuals are shown in the bottom plot.

of measurements. The smaller the deadband, the more frequent and, thus, also less “delayed” the measurements are.

Along with the system dynamic simulation, the simulated measurements o_s are collected. Then, the proposed index J_p is computed. The simulated measurements o_s are also used as an input to a traditional static WLS state estimation involving orthogonal factorization [15] yielding \hat{v} . The evolution of the objective function value of the state estimator and the proposed measure is shown in Fig. 4. Number of iterations needed for SE to converge has increased from 25 prior to the disturbance to 55 at the peak of the transients and about 35 in the end of the simulation. A strict convergence criterion was applied: a first norm of the states updates $|\Delta v| < 10^{-6}$.

To demonstrate the applicability of the proposed index J_p , we show in this example an additional measure J_r showing weighted deviation of the *estimates* from the actual conditions

$$J_r = \sum_{s=1}^S W_s (h_s(v) - h_s(\hat{v}))^2. \quad (11)$$

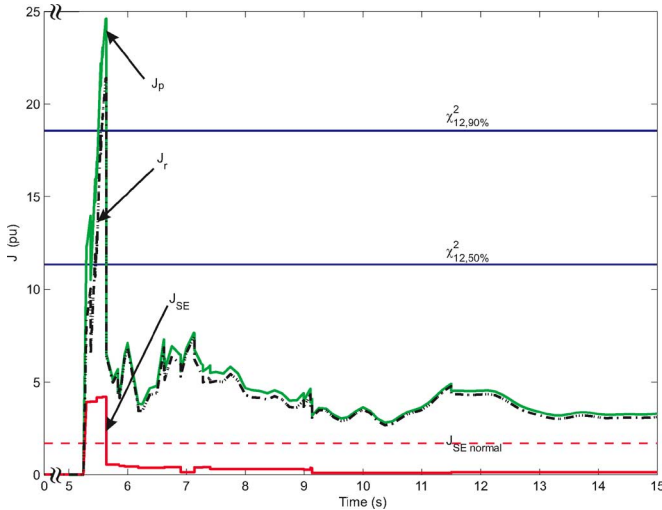


Fig. 4. Behavior of the state estimation during transient conditions: comparison of the objective functions of the state estimation and the proposed measure.

For the comparison, several further indicators are shown. The expectation of (9) for the normally distributed measurements $N(0, 1\%)$ with the standard deviation of the error $\sigma = 1\%$ is shown by $J_{SE \text{ normal}}$. The presence of the bad data in the sample shall be detected by the χ^2 tests. Since there are 17 states and 29 measurements, 12 degrees of freedom are allowed. The interpretation of, for example, 90% confidence interval is the following: objective function $J > \chi_{90\%}^2$ suggests that with 90% probability, test sample contains bad data.

Even under assumption that the topology change is instantaneously corrected in the model, all the indices show higher values due to the transients and errors introduced by the measurement chain. It can be concluded that there is a small difference between J_r , showing bad estimates and the computationally less intensive J_p . However, J_{SE} does not reflect fully the decrease of the estimator quality. In contrast to the proposed measure for the performance evaluation in dynamic conditions, J_{SE} does not exhibit very high values, since it “misses” to capture transients and operates with step-wise increasing values. In fact, J_{SE} would pass even such low as 50% confidence test for the bad data detection, while χ^2 test on J_p indicates that the measurement sample contains bad data with 90% confidence in the seconds following the disturbance. That may lead to the situation when SE fails to show that the obtained estimates are not reliable. In the addressed example, SE converged, yet in a large system, convergence might be an issue.

Thus, the necessity to simulate SE performance in dynamic conditions and suitability of the proposed evaluation index is demonstrated.

III. TRAJECTORY SENSITIVITIES ANALYSIS

Employing the modeling framework described in the previous section, the performance of state estimation can be investigated including the impact of the supervisory and monitoring infrastructure. To assess more efficiently the impact of various parameter changes, the trajectory sensitivities approach is used [18]–[20]. These sensitivities will suggest which parameters shall be changed to achieve better performance of the state estimator.

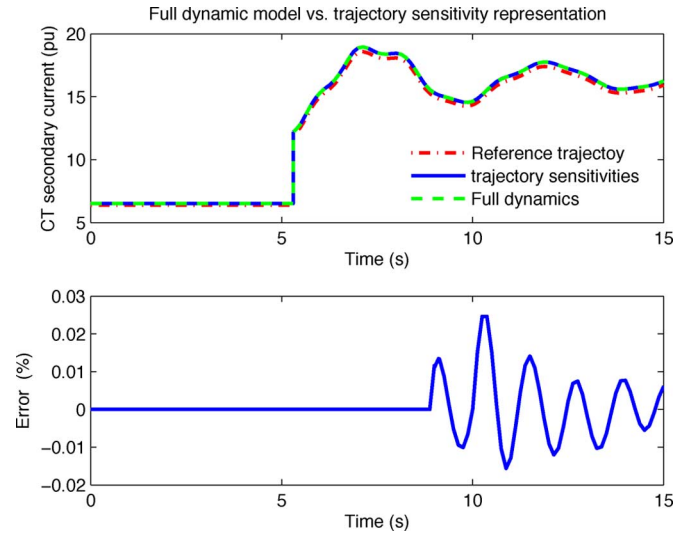


Fig. 5. Accuracy of the reproduction of the system dynamics by means of trajectory sensitivities.

Flow (i.e., time evolution) of the system from its initial point can be characterized by the time evolution of its variables [18], e.g., for algebraic variables, we can write

$$\phi_y(y_0, t) = y(t). \quad (12)$$

Trajectory sensitivities, i.e., Taylor expansion of (12), determine the impact of small changes in initial conditions on the system flow. When neglecting higher order terms, the time evolution of the algebraic states can be written as

$$\Delta y(t) = \frac{\partial y(t)}{\partial \lambda_0} \Delta \lambda_0. \quad (13)$$

The trajectory sensitivities, $(\partial y(t))/(\partial \lambda)$, are generally time varying quantities. However, the change in the parameter λ is assumed to take place in the initial point and is assumed to remain constant for the rest of the system evolution. So in our subject of application, it corresponds to a constant error or change in the analyzed parameters. This is generally true, e.g., dead-band of an RTU does not change during the operation, weight of a state estimation does not change during the operation, etc.

A numerical approximation of trajectory sensitivities can be computed by solving (1)–(6) for an incremental change of each parameter. However, that would represent a significant computational effort if many parameters are considered. The methodology for computation of trajectory sensitivities described for example in [18] involves only a minimal amount of additional computations, since it uses parts of the Jacobian evaluated when solving (1)–(6). Thus, the impact of the parameter changes on the state estimator performance can be computed efficiently.

In Fig. 5, feasibility of a very accurate approximation using trajectory sensitivities is demonstrated. Let us emphasize once again that an influence of the parameter change on the dynamic processes can be studied by running another full dynamic simulation, while trajectory sensitivity approach will provide an approximation yet requires negligible computational effort in addition to simulation of the nominal dynamic conditions.

The upper plot shows nominal trajectory with red dash-dot line; it was obtained with full dynamic time domain simulations

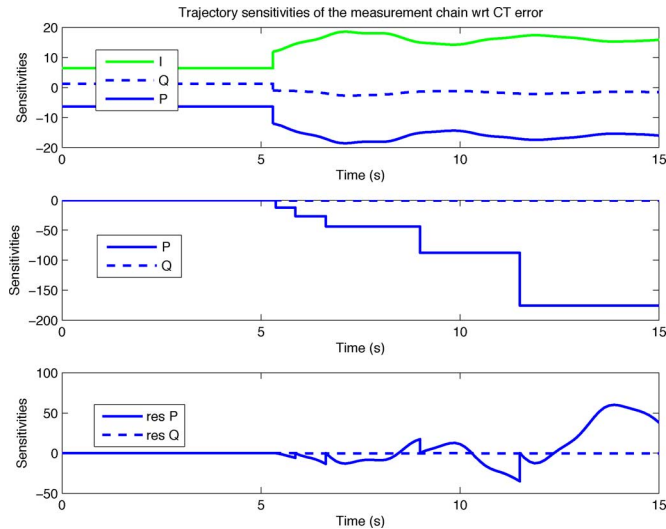


Fig. 6. Effect of the measurement error of the CT. The top picture shows the impact on the transducer, the middle picture on the RTU, and the bottom picture on the residuals of the corresponding active and reactive power flows.

for the reference system. Then, we study how the dynamic evolution of the current at the secondary side of CT would change if CT error is changed from 0 to a high value 0.02, what would correspond to a CT error class 2. The result obtained with trajectory sensitivity is compared to the exact computation of the dynamics with the new parameter. The upper plot shows both almost coinciding curves, while the bottom plot shows the difference between those. During the first 9 s of the simulation, the error of approximation is close to zero. It slightly increases afterwards.

It should be noticed that, as it is a numerical simulation, the result is a set of discrete points, but not the continuous curve. In this case, two dynamic simulations produced vector of values at slightly differing time references. That is due to slightly different instances of the discrete events, such as reaching the limits of the generators excitation system. The trajectory sensitivity vector is produced at the time instance of the nominal case. To compare the results, interpolation of the obtained values is necessary. In this case, linear interpolation was applied, which could introduce an additional error. Therefore, in the bottom plot, rather the magnitude of the error is important than the particular shape of the error.

The results of computation of the sensitivities to the different components' influences are shown in Figs. 6 and 7. Here the sensitivity is studied on the example of line (A) flows from node 5 to node 7. Several measurement chain stages are analyzed.

Fig. 6 shows from top to bottom: trajectory sensitivities of the transducer, of the RTU outputs, and of measurements residuals, i.e., of the measurements deviations from the actual conditions, with respect to the CT accuracy. The sensitivities of the transducer towards CT accuracy are continuous and somewhat constant at pre- and post- disturbance intervals.

The step-wise increase of the sensitivities in the middle plot can be explained by the deadband impact, which was shown in Fig. 3. If there was an error in the CT, RTU does not “notice” a change that should be reported and “delays” transmission of the new value. This effect accumulates in time and the sensitivity increases step-wise, as the new update is “missed”.

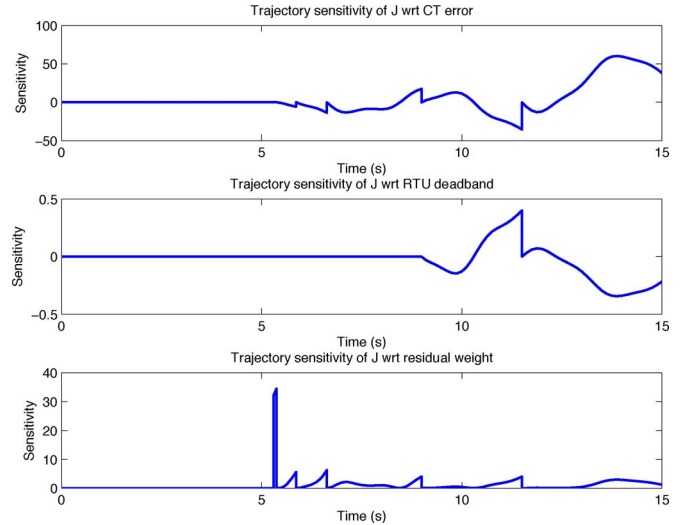


Fig. 7. Impact of various parameters of the measurement chain on the cost function J_p . Top plot—sensitivity of the J_p to the accuracy of CT, middle—sensitivity to the RTU deadband, bottom—sensitivity to the residual weight.

The sensitivity of the residual of the active and reactive power flow measurements is shown in the bottom plot. Recalling residuals presented in Fig. 3, we observe again some step-wise changes of sensitivities due to the deadbands. Sensitivity is varying as the true signal oscillates, but the value is not yet transmitted by the RTU. In addition, sensitivity increases significantly as the true signal deviates from the last transferred value.

The sensitivity of the objective function J_p to the CT error, deadband, and the weight of the current measurement is shown in Fig. 7.

The CT error seems to have the largest influence along the major part of the trajectory, while the measurement weight is playing a large role at the disturbance instant with the step change of the variables. Note that the feasible change of the parameters might be different for the different components; therefore, both the sensitivity and span of the feasible improvement of the parameter must be taken into account.

Let us take the example of the measurement of a current. If replacing a CT of the class 2 with a CT of the class 0.1, the maximum parameter change, which can be considered, equals to the difference of maximal error in these accuracy classes; thus, $\Delta\epsilon = 0.020 - 0.001 = 0.019$.

IV. GUIDING THE UPGRADE OF THE SCADA INFRASTRUCTURE

Assume there is a given limited budget, which a TSO may dedicate to upgrade the SCADA infrastructure. The objective may be to minimize the error of the state estimator during dynamic conditions by investing the upgrade budget into new RTUs. We outline below how the locations and the types of upgrades can be efficiently determined.

- 1) A set of representative system conditions together with dynamic scenarios or contingencies with corresponding weighting factors is chosen. The number of scenarios may be denoted A_{sc} and the weighting factors W_{sc} .
- 2) Scenario a is simulated for a chosen time horizon. The nominal (i.e., pre-upgrade) evolution of the corresponding

index $J_{p,na}(t)$ is stored as well as the vector of trajectory sensitivities $(\partial J_{p,na}(t))/(\partial \lambda)$. Simulations are repeated for each scenario $a \in \{1, \dots, A_{sc}\}$.

- 3) A candidate $b \in B$ from the set of possible SCADA upgrades can be expressed as an adjustment $\Delta \lambda_b$ of the corresponding parameter $\lambda_b \in L$; thus, $\Delta \lambda_b \in \Delta L$. For example, if an RTU with a smaller deadband is considered for installation, then the corresponding change of the deadband parameter is negative $\Delta \lambda_b < 0$.

Costs of individual upgrades ΔL are summarized in the vector C , whereas the upgrade for the overall upgrade would be C_{budget} .

- 4) The objective can be then expressed as

$$\min \sum_{a=1}^{A_{sc}} W_{sc,a} \int_0^T J_{p,a}(t) dt \quad (14)$$

subject to constraints

$$J_{p,a}(t) = J_{p,na}(t) + \frac{\partial J_{p,na}(t)}{\partial \lambda} \cdot \Delta L \cdot U \quad \forall a \in \{1, \dots, A_{sc}\} \quad (15)$$

$$C \cdot U \leq C_{budget} \quad (16)$$

where the solution vector U contains binary variables with entries equal to 1 for the determined upgrades and entries equal to 0 for upgrades not to be implemented, i.e., $u_b \in \{0, 1\}, \forall b \in B$.

Thus, proceeding in accordance with the described algorithm TSO can determine optimal set of the RTUs to be upgraded to improve the performance of the state estimator during the transient conditions.

V. CONCLUDING REMARKS

The paper discusses how the performance of a traditional static state estimation observing the system undergoing dynamic changes can be measured and how this information can be utilized for the improvement of the state estimation.

The necessity of such an analysis was demonstrated in the paper. For this purpose, we proposed utilization of common dynamic simulation solvers with an extension by models of the SCADA components and incorporation of additional computations of trajectory sensitivities. The discussed approach is shown to be feasible.

The performance of static estimation during the slower system transients is crucial, even critical, for a secure operation of stressed power systems. Thus, we suggest that the proposed approaches, or similar to them, shall become an integral part of engineering processes related to the commissioning and regular maintenance of the state estimation.

APPENDIX A SYSTEM DESCRIPTION

A nine-bus test system is used in this paper. Its data are available under [21] and [22]. The system is shown in Fig. 8. All the system parameters are modeled as in the base case [22], except that simple AVR model is adopted for G2-G3 as for G1, no PSS. The line (C) parameters were modified as follows: $Z = 0.003226 + j0.00695$, $B = 1.449$ pu.

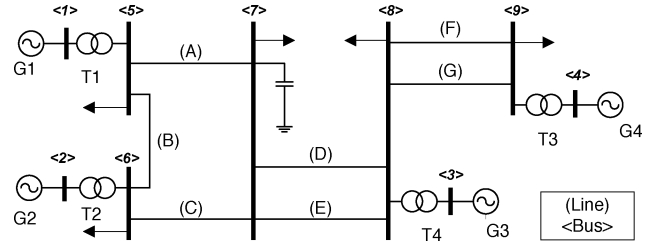


Fig. 8. Single line diagram of the nine-bus test system.

TABLE I
MEASUREMENT INFRASTRUCTURE

Bus	Location	Type
5	A, B, T1	PQ, V
6	T2, Load	PQ, V
7	D, E	PQ, V
8	F, G, T3	PQ, V
9	T4, Load	PQ, V

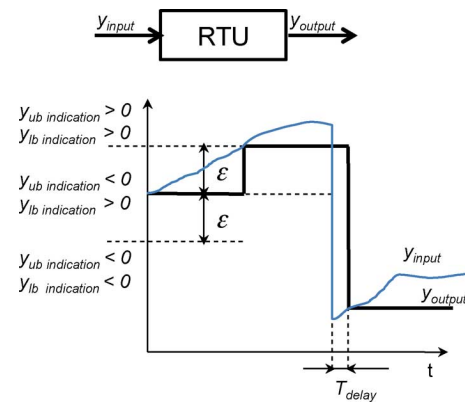


Fig. 9. Proposed model for the RTU and sampling of the signal.

The locations and types of measurements are summarized in Table I. Substations 5–9 are equipped with measurement devices and communication links; voltages are measured at all these substations and several powers.

APPENDIX B RTU MODEL

RTU is a typical representative of power system component, which creates the need for hybrid dynamics modeling in the proposed approach. RTU samples input measurement and updates according to the defined criterion the RTU output, which will be further processed in SCADA. For example, such criteria can be—a new sample is made, when the integrated input measurement deviation from the last output reaches a predefined threshold, or sampling can be carried out in regular time intervals, etc.

The framework proposed in the paper allows various degrees of complexity to be chosen for the models of the individual components. We chose a simplified model of a RTU with a single input y_{input} , a single output y_{output} , and two parameters defining the sampling—a threshold ϵ and the sample time delay T_{delay} , as in Fig. 9. This RTU updates the output, when the input measurement change from the last output exceeds the defined threshold. If the threshold is reached in a very short time,

a time delay for the measurement update is activated. To our knowledge, such delay is introduced in practice to smoothen the loading of the communication network with data packages, since a vast number of measurements shall be updated at the same time in case of a significant system change. Additional internal auxiliary variables need to be introduced into the model to apply the framework (1)–(6), so the overall RTU model becomes

$$\begin{aligned}
 \lambda_1 &: \epsilon \\
 \lambda_2 &: T_{\text{delay}} \\
 z_1 &: z_{\text{output}} \\
 y_1 &: y_{\text{input}} \\
 y_2 &: y_{\text{output}} \\
 y_3 &: y_{ub \text{ indication}} \\
 y_4 &: y_{lb \text{ indication}} \\
 y_5 &: y_{\text{timer indication}} \\
 y_6 &: y_{\text{timer}}
 \end{aligned} \tag{17}$$

where $y_{ub \text{ indication}}$ refers to the upper bound indication and $y_{lb \text{ indication}}$ to the lower bound indication, respectively. By a bound, we mean distance ϵ from the last output value.

Regardless of the hybrid dynamics, the algebraic equations apply

$$\begin{aligned}
 \lambda &: \epsilon \\
 g_1 &: 0 = y_{\text{input}} - z_{\text{output}} - \epsilon - y_{ub \text{ indication}} \\
 g_2 &: 0 = y_{\text{input}} - z_{\text{output}} + \epsilon - y_{lb \text{ indication}} \\
 g_3 &: 0 = z_{\text{output}} - y_{\text{output}} \\
 g_4 &: 0 = y_{\text{timer}} - T_{\text{delay}} - y_{\text{timer indication}}.
 \end{aligned} \tag{18}$$

At the initiation of the simulation, the output of the RTU is set equal to the input. The hybrid dynamics taking place after the initialization and during the rest of the simulation can be explained with the help of the Fig. 9. When the input measurement is smaller than $z_{\text{output}} + \epsilon$ and larger than $z_{\text{output}} - \epsilon$, the RTU output remains unchanged. In other words, when the input measurement does not deviate by more than the threshold ϵ from the last RTU output value, no update of the output is done.

Three algebraic variables of the RTU model are switching variables determining the hybrid dynamics: $y_{ub \text{ indication}}$, $y_{lb \text{ indication}}$, and $y_{\text{timer indication}}$. The update of the RTU output y_{output} takes place, when one of them equals zero, i.e., in one of the following cases:

- $y_{ub \text{ indication}} = 0$ corresponds to the situation, when the increasing input y_{input} has reached the value of the last update of the RTU output plus the threshold. In this case, the RTU output is updated according to $z_{\text{output}} = y_{\text{input}}$ and the value of the timer y_{timer} is reset to zero.
- Reaching $y_{lb \text{ indication}} = 0$ as the RTU input drops to the level of the last updated output minus threshold, results into the same consequences as in the previous case, i.e., resetting the timer and $z_{\text{output}} = y_{\text{input}}$.
- In the power system simulation environment, a signal may change significantly in a stepwise manner; thus, a measurement may exceed the threshold for the RTU output update instantaneously. In this case, one cannot determine a

unique point, where $y_{ub \text{ indication}} = 0$ or $y_{lb \text{ indication}} = 0$. Instead, the timer is triggered. As the timer value reaches the value of the predefined time delay $y_{\text{timer}} = T_{\text{delay}}$, then $y_{\text{timer indication}} = 0$, that in turn triggers the update of the RTU output $z_{\text{output}} = y_{\text{input}}$ and sets the timer to zero.

APPENDIX C NOTATION

The notation used throughout the paper is listed below for a quick reference.

Functions

f	Differential equations.
g	Algebraic equations.
h	Matrix.
h_s	Measurement function.
J	Objective function.

Variables

o	Observation, measurement.
t	Time.
x	Differential state variables.
y	Algebraic state variables.
v	Bus voltage angles and magnitudes.
\hat{v}	Estimated voltage variables.
y_d	Auxiliary variables defining changes in of g .
y_e	Auxiliary variables defining switching of the z .
z	Discrete state variables.
x^- , y^- , z^-	State variables prior to the event.
x^+ , y^+ , z^+	State variables after the event.
x_0 , y_0 , z_0	Value at the initial time instant.

Constants

a	Contingency scenario.
A_{sc}	Number of scenarios.
b	Upgrade candidate.
λ_0	Initial parameters.
λ	Parameters.
d	Number of structural changes.
e	Number of switchings of discrete variables.
m	Dimensions of the algebraic states.
l	Dimensions of parameters space.
k	Dimensions of discrete states.
n	Dimensions of dynamic states.
T	Considered time interval.
C_{budget}	Upgrade budget.
S	Measurement number.

Sets, Vectors

B	Set of candidate upgrades.
C	Upgrade cost.
D	Matrix.
E	Matrix.
L	Set of parameters.
U	Binary decision vector for optimal upgrades.
X	Set of dynamic state variables.
Y	Set of algebraic states.
Z	Set of discrete states.
\mathbf{R}	Space of real numbers.
W_s	Measurement weights.
W_{sc}	Scenario weights.

ACKNOWLEDGMENT

The authors would like to thank to Dr. T. Demiray, from BCP AG, for sharing his program for automatic generation of models.

REFERENCES

- [1] F. Schweppe and J. Wildes, "Power system static-state estimation, part I: Exact model," *IEEE Trans. Power App. Syst.*, vol. PAS-89, no. 1, pp. 120–125, 1970.
- [2] F. Schweppe and D. Rom, "Power system static-state estimation, part II: Approximate model," *IEEE Trans. Power App. Syst.*, vol. PAS-89, no. 1, pp. 125–130, 1970.
- [3] F. Schweppe, "Power system static-state estimation, part III: Implementation," *IEEE Trans. Power App. Syst.*, vol. PAS-89, no. 1, pp. 130–135, 1970.
- [4] N. Singh, "State estimation: Reality check and practical consideration," in *Robust Methods for Power System State Estimation and Load Forecasting: State of the Art and Prospects, Workshop*, Paris La Defence, France, May 29–30, 2006.
- [5] A. Phadke, J. Thorp, and M. Adamiak, "A new measurement technique for tracking voltage phasors, local system frequency, and rate of change of frequency," *IEEE Trans. Power App. Syst.*, vol. PAS-102, no. 5, pp. 1025–1038, 1983.
- [6] P. Bonanomi, "Phase angle measurements with synchronized clocks—Principle and applications," *IEEE Trans. Power App. Syst.*, vol. PAS-100, no. 12, pp. 5036–5043, 1981.
- [7] A. G. Phadke and J. S. Thorp, *Synchronized Phasor Measurements and Their Applications*. New York: Springer, Sep. 2008.
- [8] P. Rousseaux, T. Van Cutsem, and T. E. Dy Liacco, "Whither dynamic state estimation?," *Int. J. Elect. Power Energy Syst.* vol. 12, no. 2, pp. 104–116, Apr. 1990. [Online]. Available: <http://www.sciencedirect.com/science/article/B6V2T-481F1CK-6/2/f8ae2217e01b7292fc5eb64f74811645>.
- [9] N. Shivakumar and A. Jain, "A review of power system dynamic state estimation techniques," in *Proc. Joint Int. Conf. Power System Technology and IEEE Power India Conf. (POWERCON 2008)*, 2008, pp. 1–6.
- [10] F. Schweppe and R. Masiello, "A tracking static state estimator," *IEEE Trans. Power App. Syst.*, vol. PAS-90, no. 3, pp. 1025–1033, 1971.
- [11] H. Modir and R. A. Schlueter, "A dynamic state estimator for power system dynamic security assessment," *Automatica* vol. 20, no. 2, pp. 189–199, Mar. 1984. [Online]. Available: <http://www.sciencedirect.com/science/article/B6V21-47WTFJV-CF/2/31af597e72167d2266a7bffb8c049552>.
- [12] J. Chang, G. N. Taranto, and J. H. Chow, "Dynamic state estimation using a nonlinear observer for optimal series-capacitor switching control," *Int. J. Elect. Power Energy Syst.* vol. 19, no. 7, pp. 441–447, Oct. 1997. [Online]. Available: <http://www.sciencedirect.com/science/article/B6V2T-3SP79W1-3/2/7884f3ae6b0070f5fa8e1f6e25375d12>.
- [13] E. Scholtz, "Observer-based monitors and distributed wave controllers for electromechanical disturbances in power systems" Ph.D. dissertation, Dept. Elect. Eng. Comput. Sci., Massachusetts Inst. Technol., Cambridge, 2004. [Online]. Available: <http://dspace.mit.edu/handle/1721.1/26723>.
- [14] A. Monticelli, *State Estimation in Electric Power Systems: A Generalized Approach*. Norwell, MA: Kluwer, 1999.
- [15] A. Abur and A. G. Exposito, *Power System State Estimation*. New York: Marcel Dekker, 2004.
- [16] R. Minguez and A. Conejo, "State estimation sensitivity analysis," *IEEE Trans. Power Syst.*, vol. 22, no. 3, pp. 1080–1091, Aug. 2007.
- [17] S. Carullo and C. Nwankpa, "Experimental validation of a model for an information-embedded power system," *IEEE Trans. Power Del.*, vol. 20, no. 3, pp. 1853–1863, Jul. 2005.
- [18] I. Hiskens and M. Pai, "Trajectory sensitivity analysis of hybrid systems," *IEEE Trans. Circuits Syst. I: Fundam. Theory Appl.*, vol. 47, no. 2, pp. 204–220, 2000.
- [19] I. Hiskens and P. Sokolowski, "Systematic modeling and symbolically assisted simulation of power systems," *IEEE Trans. Power Syst.*, vol. 16, no. 2, pp. 229–234, May 2001.
- [20] I. Hiskens, "Power system modeling for inverse problems," *IEEE Trans. Circuits Syst. I: Reg. Papers*, vol. 51, no. 3, pp. 539–551, 2004.
- [21] P. M. Anderson, *Series Compensation of Power Systems*. PBLSH! Inc., Apr. 1996.
- [22] Main Page. [Online]. Available: http://psdyn.ece.wisc.edu/IEEE_benchmarks/index.htm.



Marija Zima (S'02-M'08) received the B.Sc. and Ph.D. degrees from the Riga Technical University, Riga, Latvia, in 2002 and 2007, respectively.

In 2000–2005, she was a planning engineer at the National power utility Latvenergo. In 2005, she started her Ph.D. studies at ETH Zürich. In 2010, she joined ABB Switzerland, Corporate Research.



Marek Zima (M'02-SM'10) received the M.Sc. degree from the Royal Institute of Technology (KTH), Stockholm, Sweden, in 2001 and the Ph.D. degree from ETH Zürich, Zürich, Switzerland, in 2006.

His industrial experience at ABB Switzerland, Atel Transmission and EGL includes R&D and sales support for wide area monitoring and control systems, grid economics, participation on designing rules for ancillary services and the grid code in Switzerland, as well as long-term gas trading analysis. Since November 2009, he has been Head of Strategic Grid Economics at Axpo Holding, Switzerland. Since 2005, he has been a lecturer and between 2006 and 2009 also a part-time Senior Researcher at ETH Zürich.



Göran Andersson (M'86-SM'91-F'97) received the M.S. and Ph.D. degrees from the University of Lund, Lund, Sweden, in 1975 and 1980, respectively.

In 1980, he joined ASEA:s, now ABB, HVDC division, and in 1986, he was appointed full Professor in electric power systems at the Royal Institute of Technology (KTH), Stockholm, Sweden. Since 2000, he has been a full Professor in electric power systems at the Swiss Federal Institute of Technology (ETH), Zürich, Switzerland, where he heads the powers systems laboratory.

Dr. Andersson is a member of the Royal Swedish Academy of Engineering Sciences and Royal Swedish Academy of Sciences.